IFSCC 2025 full paper (IFSCC2025-420)

"Preparation and Characterization of Retinol-Loaded Mannosylerythritol Lipid Nanoliposome and Its Effects on Ex Vivo Human Skin Penetration"

Han-woong Park [1], Dae-Sung Yoo [1], Chan Jin Jeong [1] and Soo Nam Park [2,*]

[1] ASK Company Co., Ltd., 86 Dongdaegu-ro, Suseong-gu, Daegu, Republic of Korea;
[2] Cosmetic Engineering, Department of Biohealth Convergence, College of Science and Convergence Technology, Seoul Women's University, 621 Hwarang-ro, Nowon-gu, Seoul 01797, Republic of Korea

1. Introduction

The skin is composed of the epidermis, dermis, and subcutaneous fat layer, and the epidermis is divided into four layers: the basal layer, stratum spinosum, granular layer, and stratum corneum. In the epidermis, there are melanocytes that synthesize melanin in addition to keratinocytes. In the dermis, there are fibroblasts that express matrix metalloproteinase (MMP), which participates in the production or degradation of extracellular matrix components such as collagen. The stratum corneum plays an important role as the skin's barrier. In particular, a series of biochemical processes in the maturation and desquamation of the stratum corneum are crucial for the skin's hydration and barrier function [1-2].

For a drug or active ingredient to be absorbed by the skin, it must first pass through the outermost layer of the epidermis—the stratum corneum. However, the stratum corneum functions as a barrier preventing the absorption of external substances, making penetration difficult. Therefore, it is considered necessary to develop transdermal delivery systems (TDDSs) such as liposomes using various physicochemical techniques and performing formulation studies to enhance the skin permeation of drugs and functional materials [3].

Liposomes are being investigated in cosmetics to examine the efficacy of functional materials on the skin. These materials may have antioxidant properties, help with anti-aging (wrinkle improvement), suppress hyperpigmentation (whitening), and improve skin barrier function. Additionally, TDDSs are being developed to make products more stable. The TDDSs developed by the authors and fellow researchers include liposomes for enhancing transdermal absorption, such as ethosomes [4]. elastic liposomes [5], cationic liposomes [6], cell-penetrating peptide liposomes [7], hydrogels [8], cyclodextrin in liposomes [9], and liposomes in hydrogel [10]; liposomes for improving the stability of materials and liposome formulations, such as multilayer liposomes [11], liposome core capsosomes [12], solid lipid nanoparticles [13], and nanostructured lipid carriers [14], and environment-responsive specialized formulations such as pH-sensitive hydrogels [15], pH-sensitive liposomes [11], pH- and temperature-sensitive hydrogels [16], and reactive oxygen species (ROS)-sensitive nanoparticles [17].

In the early 1990s, conventional liposomes made from phosphatidylcholine were repeatedly found to be nearly incapable of overcoming the skin permeability barrier. Therefore, Cevc and Blume added a bilayer softening component known as an “edge activator,” specifically a biocompatible surfactant, to liposomes to increase the lipid flexibility and permeability of the vesicles and referred to these liposomes as “deformable liposomes” [18]. In this study, mannosylerythritol lipid (MEL) was used as the edge activator for deformable liposomes. MEL—a biosurfactant produced by the microorganism Candida sp. SY16— has the full name 6-O-acetyl-2,3-di-O-alkanoyl-β-D-mannopyranosyl-(1→4)-O-meso-erythritol [19].

The active ingredient used in the present study is retinol. Retinoids—a group of vitamin A derivatives—are among the most extensively researched ingredients in skincare for preventing aging and enhancing the appearance of mature skin. In South Korea, retinol is used as an anti-wrinkle agent in functional cosmetics [20]. It can stimulate collagen synthesis, inhibit MMP activity, reduce oxidative stress, and regulate gene expression [21]. Retinol has also shown efficacy in improving the visual signs of intrinsic and extrinsic aging, such as wrinkles and irregular pigmentation.

In this study, the MEL biosurfactant was used as an edge activator to produce deformable liposomes (or elastic liposomes) that encapsulate retinol, which is a functional substance for anti-aging and wrinkle improvement. The physicochemical properties of the manufactured deformable liposomes, such as the zeta potential, storage stability, encapsulation efficiency, and deformability index, were verified using particle size and zeta potential analysis, UV-vis spectrophotometry, mini-extrusion, and cryogenic transmission electron microscopy (cryo-TEM). We also used a Franz cell diffusion system to examine the depth, and amount of skin penetration by the retinol in the deformable liposome. The results indicated that the optimal MEL-liposome formulation selected in this study is highly effective transdermal drug delivery system (TDDS), with potential applicability for delivering cosmetic functional materials, such as retinol, in cosmetics.

2. Materials and Methods

2.1 Materials

MEL was obtained from LABIO Co., Ltd. (Seoul, Korea), and hydrogenated lecithin (HL) was purchased from Lipoid GmbH (Germany). Cer was obtained from Doosan Co., Ltd. (Seoul, Korea). Cholesterol was obtained from Active Concepts (Lincolnton, North Carolina, USA). Retinol was obtained from BASF (Ludwigshafen, Germany). Chloroform and methanol of analytical grade were purchased from JT Baker (Phillipsburg, New Jersey, USA).

2.2 Preparation of MLs

MEL-liposomes (MLs) were prepared via a thin-film hydration method. The various formulations consisting of HL, MEL, Cer, Chol, and retinol are presented in Table 1.

Table 1. Compositions of the MLs

Formulation code (HL:MEL mass ratio)	Composition (%, w/v)				
	HL	MEL	Cer	Chol	Retinol
ML-1 (10:0)	0.5	-	0.005	0.1	0.05
ML-2 (7:3)	0.35	0.15	0.005	0.1	0.05
ML-3 (5:5)	0.25	0.25	0.005	0.1	0.05
ML-4 (3:7)	0.15	0.35	0.005	0.1	0.05
ML-5 (0:10)	-	0.5	0.005	0.1	0.05

Five MEL-liposome formulations (ML-1 to ML-5) were prepared with varying weight ratios of hydrogenated lecithin, a phospholipid, and MEL (used as an edge activator), as shown in Table 1. As listed in Table 1, all ingredients were dissolved in a chloroform/methanol mixture (5/5 v/v, 60 mL), and then, the solvents were removed using a rotary evaporator (IKA, Germany) to form a lipid film. This lipid film was hydrated with distilled water in an ultrasonic bath (Kudos, China) to prepare a lipid suspension. This lipid suspension was treated with a microfluidizer (Micronox, Korea) and filtered through a 0.45 μm filter (Minisart CA 26 mm) to obtain the final liposome solution, which was used in the experiment.

2.3 Analysis of particle size and zeta potential

The particle-size distribution and zeta potential of the MLs were measured using a particle-size analyzer (Litesizer DLS, Anton Paar, Austria) and a zeta-potential analyzer (Zetasizer Nano ZS, Malvern Instruments, United Kingdom), respectively. The average particle size was calculated using cumulative analysis, and the particle distribution was analyzed using the CONTIN algorithm [3]. The MLs were analyzed at 25 ℃, and all measurements were performed in triplicate.

2.4 Encapsulation efficiency of MLs

The liposomes (1 mL, 10 mg/mL) were purified via 0.45 μm filtration to remove unencapsulated retinol. Subsequently, an excess amount of ethanol was added to dissolve the retinol contained within the filtered liposomes. After the ethanol was completely removed by a rotary evaporator, the sample was redissolved in ethanol (1 mL). The retinol content in the MLs was measured at its maximum absorption wavelength of 325 nm using a UV-visible (UV-vis) spectrometer, and a calibration curve for retinol concentration was created using a standard solution. The concentration of the loaded retinol was then calculated, and the calculated value was substituted into the following Equation (1) to determine the entrapment efficiency.

$$\text{Entrapment efficiency (\%)} = C_e/C_i \times 100 \qquad (1)$$

Here, C_i represents the initial concentration of retinol (mg/mL), and C_e represents the concentration of loaded retinol (mg/mL).

2.5 Evaluation of deformability index of MLs

To evaluate the deformability index of the prepared MLs, the degree of deformation when passing through an artificial permeation barrier was measured using a mini extruder (Avanti Polar Lipids). MLs were extruded through a polycarbonate membrane with a pore size of 50 nm at a pressure of 0.2 MPa for 1 min, and the amount of ML solution passing through the membrane was recorded. Additionally, the size of ML particles that passed through the membrane was measured. The deformability index of the ML membrane was determined using Equation (2): [22]

$$\text{Deformability index} = J_{Flux} \times (r_v/r_p)^2 \qquad (2)$$

where J_{Flux} (mg/cm^2/s) is the rate of nanoliposome mass transfer across the membrane per unit area over time, r_v is the particle size of the nanoliposome after extrusion (nm), and r_p is the pore size of the membrane (nm).

2.6 Cryo-TEM

A cryogenic transmission electron microscope (cryo-TEM; Cryo Tecnai F20, FEI Company, USA, 200 kV) was used to observe the morphology of the prepared deformable liposomes.

The liposome bilayer thickness was calculated using the scale bar in the acquired cryo-TEM image.

2.7 *In vitro* skin permeation using Franz diffusion cells

In vitro skin penetration studies of retinol-loaded deformable liposomes were conducted using a Franz diffusion cell (DHC-6TD, Logan Instruments, USA). Whole skin (Seedgroup Co., Ltd., Korea) from a 77-year-old male donor was used with the donor's consent. After 24 h, the skin surface was washed with PBS to measure the amount of retinol contained within the stratum corneum and deeper skin layers, and the stratum corneum was removed by stripping three times using Scotch tape (3M, Maplewood, MN, USA). Afterward, the collected tape and retinol on the skin were dissolved by sonication in 100% ethanol. The concentration of the recovered retinol was measured using a UV-vis spectrophotometer [1, 10].

2.9. Statistical Processing

Experiments were conducted in triplicate, and statistical data were expressed as mean ± SD. Statistical significance was evaluated using the GraphPad Prism 7.0 software (San Diego, CA) via one-way ANOVA, with significance levels set at $p < 0.05$ and $p < 0.01$.

3. Results

3.1 Particle size, PDI, and zeta potential of MLs

MLs were prepared using HL and MEL at mass ratios of 10:0, 7:3, 5:5, 3:7, and 0:10, and these formulations were designated as ML-1, ML-2, ML-3, ML-4, and ML-5, respectively (Table 1). The measurement results for the particle size, polydispersity index (PDI), and zeta potential of the MLs are presented in Table 2. The average particle sizes of ML-1, ML-2, ML-3, ML-4, and ML-5 were measured as 137.0 ± 34.4, 79.5 ± 14.4, 87.5 ± 10.9, 89.3 ± 6.8, and 181.2 ± 54.3 nm, respectively. The deformable liposomes (ML-2, ML-3, and ML-4) had smaller particle sizes than the normal liposome (ML-1) and MEL liposome (ML-5), and the average particle size was <100 nm.

If the PDI of liposomes is <0.3, they have good size homogeneity [23]. The PDI values of ML-1, ML-2, ML-3, ML-4, and ML-5 were 0.249 ± 0.0304, 0.268 ± 0.006, 0.271 ± 0.008, 0.263 ± 0.012, and 0.226 ± 0.055, respectively. As the PDI was <0.3 for all the ML formulations, the particle distribution exhibited monodispersity, indicating that the liposome particle size was homogeneous.

Generally, liposome suspensions with a zeta potential of +30 mV or higher or –30 mV or lower are considered stable. Furthermore, the zeta potential is related to the charge on the vesicle surface, which affects not only the stability of the liposomes but also their properties and their interaction with the skin. All the formulations prepared in this study (n = 3) exhibited negative zeta potentials: –32.9 ± 6.6 mV for ML-1 (the normal liposome), –27.6 ± 1.9 mV for ML-2, –26.7 ± 2.3 mV for ML-3, –25.2 ± 1.1 mV for ML-4, and –8.1 ± 0.5 mV for ML-5 (MEL alone). As expected, owing to the ionic nature of the HL hydrophilic head, the normal liposome (ML-1) composed solely of lecithin exhibited the most negative zeta potential (–32.9 ± 6.6 mV) among the liposome formulations, while the zeta potentials of ML-2, ML-3, and ML-4, with decreasing lecithin ratios, exhibited a decreasing trend. ML-5, corresponding to standalone MEL with a nonionic hydrophilic group and without lecithin having an ionic hydrophilic group, exhibited a low zeta potential (–8.1 ± 0.5 mV), as expected.

Table 2. Formulation of liposomes with different average particle sizes, PDIs, and zeta potentials.

Formulation code (HL:MEL mass ratio)	Size (nm)	PDI	Zeta potential (mV)
ML-1 (10:0)	137.0 ±34.4*	0.249 ±0.034*	–32.9 ±6.6*
ML-2 (7:3)	79.5 ±14.3**	0.268 ±0.006**	–27.6 ±1.9**
ML-3 (5:5)	87.5 ±10.9**	0.271 ±0.008**	–26.7 ±2.3**
ML-4 (3:7)	89.3 ±6.8**	0.263 ±0.012**	–25.2 ±1.1**
ML-5 (0:10)	181.2 ±54.3*	0.226 ±0.055*	–8.1 ±0.5*

*P < 0.05; **P < 0.01

3.2 Stabilization of MLs

The stability of the MLs was assessed by comparing the particle sizes immediately after manufacture and after 4 weeks of storage (Figure 1). The measured changes in the average particle size after four weeks were as follows: ML-1, reduction from 137.0 to 124.7 nm; ML-2, reduction from 79.5 to 77.6 nm; ML-3, reduction from 87.5 to 77.3 nm; ML-4, reduction from 89.3 to 81.7 nm; ML-5, increase from 181.2 to 316.7 nm. ML-1, ML-2, ML-3, and ML-4 exhibited slight reductions in average particle size after 4 weeks but maintained particle sizes similar to those immediately after manufacture, indicating relatively high stability. However, ML-5 was discovered to be an unstable formulation, with the average particle size increasing by a factor of approximately 1.5 over 4 weeks.

3.3 Encapsulation efficiency of retinol in ML

The retinol encapsulation efficiency of liposome formulations according to the HL:MEL mass ratio is shown in Figure 2. The encapsulation efficiencies of ML-1, ML-2, ML-3, ML-4, and ML-5 were measured as 67.1 ± 10.1%, 86.3 ± 2.5%, 87.9 ± 1.4%, 86.3 ± 2.3%, and 82.1 ± 2.9%, respectively.

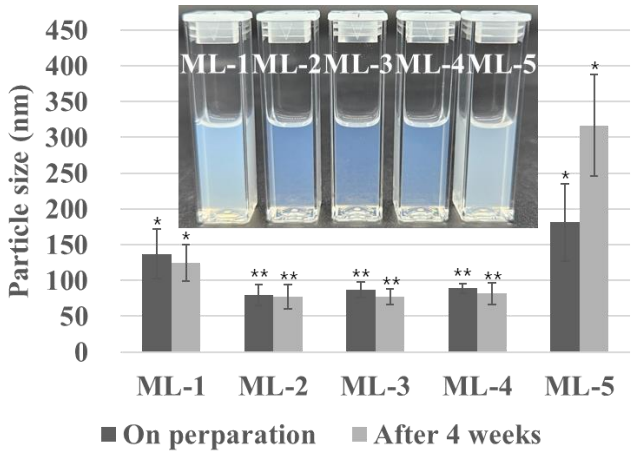

Figure 1. Stability of the particle size of the MLs after 4 weeks. The inset shows the physical appearance of the samples upon preparation. *P < 0.05; **P < 0.01.

The encapsulation efficiency of the active ingredients in liposomes is affected by the surfactant used [24]. The normal liposome ML-1, which was manufactured solely with HL, exhibited the lowest encapsulation efficiency, whereas the deformable liposomes (ML-2, ML-3, and ML-4) manufactured with HL and MEL exhibited encapsulation efficiencies of >85%. When MEL and HL are present in a mixed ratio, the solubility of retinol is higher than that of HL alone, suggesting that the content of retinol in the elastic liposome has increased.

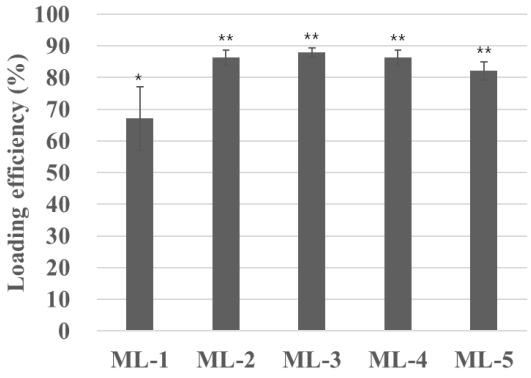

Figure 2. Encapsulation efficiencies of MLs containing retinol. *P < 0.05; **P < 0.01.

3.4 Deformability indices of MLs

The deformability indices were measured to evaluate the deformability of the MLs (Table 3). The deformability index was measured as 2.44 ± 1.1 for ML-1, 3.24 ± 1.4 for ML-2, 3.88 ± 0.8 for ML-3, 5.76 ± 1.9 for ML-4, and 27.38 ± 6.5 for ML-5. Conventional liposomes without edge activators have limitations in penetrating the skin [25]. The edge activator makes the lipid bilayer of deformable liposomes more flexible, increasing their deformability. As mentioned previously, the normal liposome ML-1 exhibited the lowest deformability among the liposomes we tested. Furthermore, it was confirmed that as the mass ratio of MEL used as an edge activator increased to 30%, 50%, and 70%, the deformability increased. We consider that the increase in the MEL ratio transformed the liposome membrane from a rigid membrane into a flexible membrane, increasing the deformability. Among the aforementioned HL:MEL ratios, 3:7 (corresponding to ML-4) yielded the highest deformability index. The measured physical properties indicated that the ML-4 formulation, with an HL:MEL mass ratio of 3:7, had a uniform particle size, a high absolute zeta potential, stability during the storage period, a high encapsulation efficiency of retinol, and a high deformability index.

Table 3. Deformability indices of the MLs.

Formulation code	Deformability index
ML-1	2.44 ± 1.1*
ML-2	3.24 ± 1.4**
ML-3	3.88 ± 0.8**
ML-4	5.76 ± 1.9**
ML-5	27.38 ± 6.5*

*P < 0.05; **P < 0.01.

3.5 Morphological analysis of ML

Figure 3 shows the structure of the MLs as observed using cryo-TEM. Figure 3a presents a cryo-TEM image of ML-1, showing the dense bilayer and uniform spherical shape of phospholipid liposomes. ML-4 also exhibited a typical liposome bilayer and a spherical membrane structure with a thinner bilayer than ML-1 (Figure 3b). ML-5, which was made entirely of MEL, had both a liposome bilayer and multilayer structures, as well as particles of varying sizes and unstable, aggregated forms, in contrast to ML-1 and ML-4 (Figure 3c). Furthermore, the thickness of the liposome bilayer observed in cryo-TEM was approximately 4–5 nm for ML-1, 3.5–4.5 nm for ML-4, and 2.5–3.5 nm for ML-5.

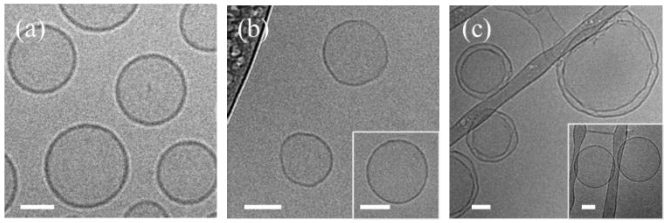

Figure 3. Cryo-TEM images of (a) ML-1, (b) ML-4, and (c) ML-5 (the scale bars represent 50 nm).

3.6 *In vitro* Franz diffusion cell skin permeation of MLs

In this study, a deformable liposome TDDS using MEL as an edge activator was developed to enhance the skin absorption of retinol, which is known as an anti-wrinkle agent in functional cosmetics (Figure 4 and 5). In the experiment, ML-4 (HL:MEL = 3:7), which was selected as the optimal formulation, ML-1 consisting only of HL, and a retinol solution dissolved in 1,3-BG as a control group were used. Figure 4 presents the measured amounts of retinol in the 1,3-BG, ML-1, and ML-4 formulations that passed through the skin (transdermal) at different time points (0, 1, 3, 6, 12, 24 h). As shown, ML-4 had the highest skin permeation rate of retinol at 24 h (12.1%), followed by ML-1 (6.9%) and 1,3- BG (0.2%) at 24 h.

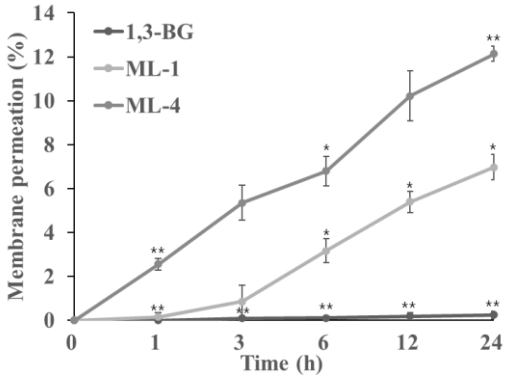

Figure 4. *In vitro* skin permeation profiles of the 1,3-BG solution and ML-1 and ML-4 containing retinol over 24 h. *P < 0.05; **P < 0.01.

Figure 5 shows the amount of retinol for each formulation and in the stratum corneum (Tape), skin layer (Skin; epidermis + dermis), and transdermal (Transdermal) 24 hours after applying each formulation to the skin. Figure 5a shows the amount of retinol present in the stratum corneum (Tape), the amount present in the epidermis and dermis excluding the stratum corneum (Skin), and the amount that penetrated the skin (Transdermal) (Figure 5). After 24 h of skin application, the amount of retinol absorbed and present in the stratum corneum (Tape) was 1.0 %, 3.1 %, and 4.1 % for the 1,3-BG, ML-1, and ML-4 formulations, respectively. Thus, the amount absorbed into the stratum corneum was the largest for ML-4. The amount of retinol that permeated into the epidermis and dermis (Skin) was also the largest for ML-4; it was 2.2, 8.3, and 12.8 % for 1,3-BG, ML-1, and ML-4, respectively. Finally, the amount of retinol that penetrated the skin (Transdermal) was 0.2, 7.0, and 12.1 % for 1,3-BG, ML-1, and ML-4, respectively. Thus, the ML-4 formulation showed the largest amount of retinol that completely penetrated the skin (transdermal). In the case of ML-4 deformable liposomes, the amount of retinol absorbed into the skin layer was similar to the amount of transdermal retinol.

Figure 5b shows the combined amount of retinol in the stratum corneum (Tape), skin layer (Skin), and transdermal (Transdermal), as represented in Figure 5a The total skin penetration

of retinol for the 1,3-BG, ML-1, and ML-4 formulations was 3.4%, 18.4%, and 29.0%, respectively. Among these, the ML-4 deformable liposome showed the highest skin penetration due to its small particle size, high encapsulation efficiency, and flexible liposome membrane. Compared with the normal liposome (ML-1) using only lecithin without MEL, ML-4, which used MEL as an edge activator and had an HL:MEL mass ratio of 3:7, exhibited 4.5 % greater skin permeation in the skin layer (Skin = epidermis + dermis) and 5.1 % greater skin transit of retinol (Transdermal) (Fig. 5).

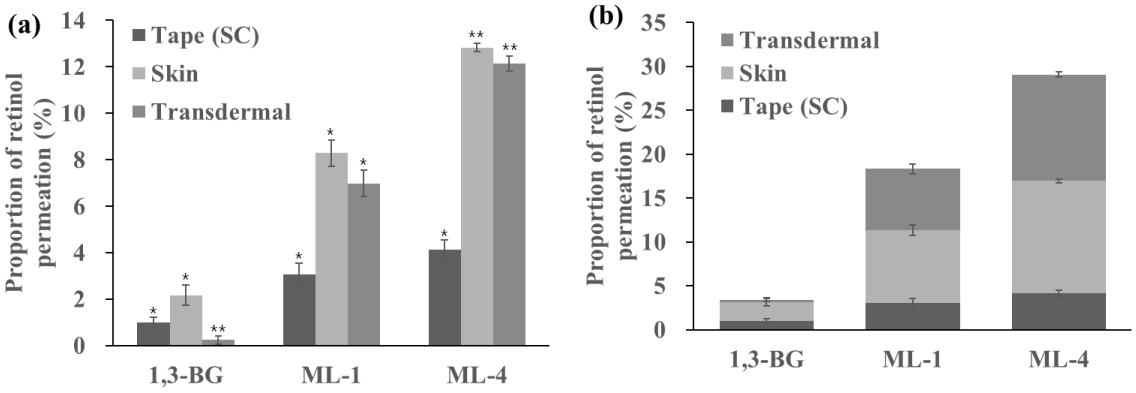

Figure 5. Proportions of the permeated amount of the 1,3-BG solution and ML-1 and ML-4 containing retinol through human skin after 24 h of incubation (Tape: stratum corneum, Skin: epidermis without stratum corneum plus dermis, Transdermal: receptor chamber). *P < 0.05; **P < 0.01.

4. Discussion

Delivering anti-aging materials such as wrinkle-improving compounds, deep into the skin remains a significant challenge. Delivering functional materials to the epidermis and/or dermis without physical damage to the skin is crucial in cosmetics. For a drug or active ingredient to be absorbed by the skin, it must first pass through the outermost layer of the epidermis—the stratum corneum. However, the stratum corneum functions as a barrier preventing the absorption of external substances, making penetration difficult. Therefore, it is considered necessary to develop transdermal delivery systems (TDDSs) such as liposomes, that can more easily pass through the stratum corneum using various physicochemical techniques and performing formulation studies to enhance the skin permeation of functional materials.[3]

In this study, we prepared deformable liposomes encapsulating retinol, an anti-aging and wrinkle-improving functional material, using MEL biosurfactant as an edge activator. MEL-liposomes (ML) were prepared with mass ratios of HL and MEL, and these formulations were designated ML-1 to ML-5, respectively (Table 1). The measurement results for the particle size, polydispersity index (PDI), and zeta potential of the MLs are presented in Table 2. The deformable liposomes (ML-2, ML-3, and ML-4) had smaller particle sizes than the normal liposome (ML-1) and MEL liposome (ML-5), and the average particle size was 85.4±10.7 nm, with all particles being <100 nm in size. As the PDI was <0.3 for all the ML formulations, the particle distribution exhibited monodispersity, indicating that the liposome particle size was homogeneous. The particle size of the deformable liposomes is small and stable even in a wide range of HL:MEL weight ratios (7:3 to 3:7).

The encapsulation efficiency of the active ingredients in liposomes is affected by the surfactant used [24]. The normal liposome ML-1, which was manufactured solely with HL, exhibited the lowest encapsulation efficiency, whereas the deformable liposomes (ML-2, ML-3, and ML-4) manufactured with HL and MEL exhibited encapsulation efficiencies of >85%. In particular, the hydrophobic fatty acid chains of MEL are predominantly composed of hexanoic acid (49 mol%),

dodecanoic acid (23 mol%), tetradecanoic acid (19 mol%), and the unsaturated fatty acid tetradecenoic acid (9 mol%) [23]. Thus, the chain length of MEL is far shorter than the average fatty acid chain length of HL used in liposome preparation. MEL can increase the encapsulation efficiency of lipid components such as retinol by providing a flexible space in the rigid lipid bilayer membrane of liposomes composed solely of HL. Therefore, the encapsulation efficiencies of ML-3 and ML-4, which were composed of HL, were 87.9% and 86.3% respectively, indicating that ML had an approximately 20% higher encapsulation efficiency than the normal liposome.

The normal liposome ML-1 exhibited the lowest deformability among the liposomes we tested. Furthermore, it was confirmed that as the mass ratio of MEL used as an edge activator increased, the deformability increased. Among the HL:MEL ratios, ML-4 with a ratio of 3:7 showed the highest deformability index (Table 3)

The measured physical properties indicated that the ML-4 formulation, with an HL:MEL mass ratio of 3:7, had a uniform particle size, a high absolute zeta potential, stability during the storage period, a high encapsulation efficiency of retinol, and a high deformability index. Therefore, ML-4 was selected as the optimal deformable liposome formulation.

To investigate how the developed delivery system affects the skin absorption rate compared with the existing delivery system, the in vitro skin permeation ability was evaluated using a Franz diffusion cell (Figure 4 and 5). In the experiment, ML-4 (HL:MEL = 3:7), which was selected as the optimal formulation, ML-1 consisting only of HL, and a retinol solution dissolved in 1,3-BG as a control group were used. ML-4 had the highest skin permeation rate of retinol at 24 h (12.1%), followed by ML-1 (6.9%) and 1,3-BG (0.2%) (Figure 4). The total skin penetration of retinol for the 1,3-BG, ML-1, and ML-4 formulations was 3.4%, 18.4%, and 29.0%, respectively. Among these, the ML-4 deformable liposome showed the highest skin penetration due to its small particle size, high encapsulation efficiency, and flexible liposome membrane. The addition of MEL between the lipid bilayers not only increased the lipid bilayer flexibility but also introduced MEL-derived fatty acids, which are shorter than the phospholipid fatty acid chains. This structural modification facilitated liposome fusion with biological membranes and enhanced drug penetration efficiency owing to their ability to efficiently encapsulate drugs such as retinol.

In this experiment, the retinol used as a functional material exhibits anti-aging activity such as wrinkle improvement by stimulating collagen synthesis in the dermis, inhibiting MMP expression, and reducing oxidative stress. Additionally, its derivative RA has been reported to inhibit excessive pigmentation by downregulating the expression of tyrosinase—a key enzyme in melanin synthesis—in melanocytes located in the basal layer of the epidermis and thereby inhibiting melanin production and the transfer of melanosomes to keratinocytes. Therefore, this MEL-deformable liposome formulation (ML-4) allowed 24.9% of retinol to pass through the skin (skin + transdermal), efficiently delivering retinol to the skin layer at a content that was 9.6% greater than the relative penetration amount of 15.3% for the conventional liposome (ML-1). It is believed that using this MEL-deformable liposome as a TDDS can induce anti-aging effects such as wrinkle improvement as well as whitening effects that inhibit hyperpigmentation.

5. Conclusion

In this study, to enhance the skin absorption of retinol, a functional cosmetic ingredient known for its wrinkle-improving properties, deformable liposome formulations loaded with retinol were prepared using hydrogenated lecithin and MEL as an edge activator at weight ratios of HL:MEL = 10:0, 7:3, 5:5, 3:7, and 0:10. Among the five formulations (ML-1 to ML-5), ML-4, with a weight ratio of HL:MEL = 3:7, was identified as the optimal deformable liposome formulation based on these characteristics. The morphological structure of the liposome was examined using cryo-TEM, comparing ML-4 with the conventional liposome ML-1 (without MEL) as a control.

The skin penetration ability of retinol in each formulation was evaluated. Cryo-TEM observations confirmed that ML-4 maintained a stable liposome membrane with a distinct lipid bilayer, similar to ML-1. The retinol skin penetration ability of the ML-4 deformable liposome formulation was more than 10% higher than that of the conventional liposome (ML-1). These results indicate that the the retinol loaded ML-4 deformable liposome formulation significantly enhances the skin penetration and absorption of functional cosmetic ingredients. Therefore, this formulation shows strong potential for sustainable applications in cosmetics and the development of TDDS platforms for functional skincare.

6. References

1. A. R. Kim, N. H. Lee, Y. M. Park, S. N. Park, J. Drug Deliv. Sci. Technol. 2019, 52, 150.
2. R. Voegeli, A. V. Rawlings, Int. J. Cosmet. Sci. 2023, 45(2), 133.
3. S. J. Kim, S. S. Kwon, S. H. Jeon, E. R. Yu, S. N. Park, Int. J. Cosmet. Sci. 2014, 36(6), 553.
4. H. G. Yang, H. J. Kim, H. S. Kim, S. N. Park, Appl. Chem. Eng. 2013, 24(2), 190.
5. S. H. Park, H. S. Shin, M. E. Yun, S. L. Lee, B. R. Song, N. H. Lee, S. N. Park, Polym. Korea 2018, 42(2), 330.
6. H. A. Gu, M. J. Kim, H. S. Kim, J. H. Ha, E. R. Yu, S. N. Park, Appl. Chem. Eng. 2015, 26(2), 165.
7. S. S. Kwon, S. Y. Kim, B. J. Kong, K. J. Kim, G. Y. Noh, N. R. Im, J. W. Lim, J. H. Ha, J. Kim, S. N. Park, Int. J. Pharm. 2015, 483(1), 26.
8. B. J. Kong, A. Kim, S. N. Park, Carbohydr. Polym. 2016, 147, 473.
9. N. R. Im, K. M. Kim, S. J. Young, S. N. Park, Korean J. Chem. Eng. 2016, 33(9), 2738.
10. J. H. Ha, Y. J. Jeong, A. Y. Kim, I. K. Hong, N. H. Lee, S. N. Park, Eur. J. Lipid Sci. Technol. 2018, 120(9), 1800125.
11. J. S. Seong, M. E. Yun, S. N. Park, Carbohydr. Polym. 2018, 181, 659.
12. C. Y. Yoo, J. S. Seong, S. N. Park, Colloids Surf. B Biointerfaces 2016, 144, 99–107.
13. S. B. Han, S. S. Kwon, Y. M. Jeong, E. R. Yu, S. N. Park, Int. J. Cosmet. Sci. 2014, 36(6), 588.
14. N. H. Lee, S. H. Park, S. N. Park, J. Drug Deliv. Sci. Technol. 2018, 48, 245.
15. H. J. Jeong, S. J. Nam, J. Y. Song, S. N. Park, J. Drug Deliv. Sci. Technol. 2019, 51,194.
16. A. R. Kim, S. L. Lee, S. N. Park, Int. J. Biol. Macromol. 2018, 118, 731.
17. A. Y. Kim, J. H. Ha, S. N. Park, Biomacromolecules 2017, 18(10), 3197.
18. G. Cevc, G. Blume, Biochim. Biophys. Acta BBA - Biomembr. 1992, 1104(1), 226.
19. H-S. Kim, B-D. Yoon, D-H. Choung, H-M. Oh, T. Katsuragi, Y. Tani, Appl. Microbiol. Biotechnol. 1999, 52(5), 713.
20. A. Ascenso, H. Ribeiro, H. C. Marques, H. Oliveira, C. Santos, S. Simões, Mini. Rev. Med. Chem. 2014, 14(8), 629.
21. Y. Shao, T. He, G. J. Fisher, J. J. Voorhees, T. Quan, Int. J. Cosmet. Sci. 2017, 39(1), 56.
22. S. Duangjit, Y. Obata, H. Sano, Y. Onuki, P. Opanasopit, T. Ngawhirunpat, K. Takayama, Biol. Pharm. Bull., 2014, 37(2), 239.
23. M. Badran, Dig. J. Nanomater. Biostruct. 2014, 9(1), 83.
24. M. R. Porter, Use of surfactant theory. In: Handbook of Surfactants, Springer, Boston, MA, 1991.
25. T. Imura, N. Ohta, K. Inoue, N. Yagi, H. Negishi, H. Yanagishita, D. Kitamoto, Chem. – Eur. J. 2006, 12(9), 2434.